Toughness Enhancement of Poly(ethylene terephthalate) with Functionalized Ultrahigh Molecular Weight Polyethylene

L. MASCIA, A. OPHIR*

Institute of Polymer Technology and Materials Engineering, Loughborough University, Loughborough LE11 3TU, United Kingdom

Received 3 August 2000; accepted 10 November 2000

ABSTRACT: Ultrahigh molecular weight polyethylene (UHMWPE) is available commercially in the form of powder, consisting of fine primary particles, 1–5 μm in diameter, agglomerated into secondary "free-flowing" particles with overall dimensions in the region of 50 to 150 μm. These are normally sufficiently coherent and retain their conglomerated particulate structure when blended with other polymers because of the extremely high viscosity of UHMWPE. In this study the surface of the agglomerated primary particles was acid functionalized by reactions with aqueous solutions of acrylic acid, after being irradiated with γ-radiation at 15–45 kGy. The acid groups were used to introduce a glycidoxyl functionality through reactions with a difunctional cycloaliphatic epoxy resin and also to a "partial" metal carboxylate functionality through reactions with zinc acetyl acetonate. When blended with polyethylene terephthalate (PET) in either a small-batch mixer or in a twin-screw extruder all the treated powders, except those functionalized with acrylic acid, were broken down to their primary size and were uniformly dispersed and strongly bonded to the surrounding matrix. The blends containing the deglomerated particles were found to have much greater ductility and toughness than those produced from both untreated and acid functionalized powder. © 2001 John Wiley & Sons, Inc. J Appl Polym Sci 81: 2972–2986, 2001

Key words: ultrahigh molecular weight polyethylene; poly(ethylene terephthalate); zinc acetyl acetonate; crystallization; ductility; compatibilization; toughening agent

INTRODUCTION

The main deficiencies of poly(ethylene terephthalate) (PET) for many industrial applications are the intrinsic slow crystallization from the melt and the excessive brittleness of products after crystallization. Both aspects have received considerable attention in scientific studies and for the development of industrial products.[1]

Because the crystalline form of PET (CPET) is preferred for product applications requiring dimensional stability and mechanical strength at high temperatures, there is a real need to develop toughened grades that exhibit enhanced nucleation characteristics.

Polyolefins are known to be efficient nucleating agents for PET and, therefore, their use as toughening agents is attractive for the fulfillment of the two specified requirements for high-temperature applications.[2]

Gross phase separation, however, inevitably occurs in blends of two dissimilar crystalline poly-

* *Present address:* Israel Plastics and Rubber Center, Technion City, Haifa 3200, Israel.

Correspondence to: L. Mascia (L.Mascia@lboro.ac.uk).

Contract grant sponsor: Eastman Chemical Company.

Journal of Applied Polymer Science, Vol. 81, 2972–2986 (2001)
© 2001 John Wiley & Sons, Inc.

mers as a result of their tendency to crystallize as pure components. In the majority of the cases this is accentuated by their limited miscibility in the melt state.[3] The differences in both level of supercooling required for nucleation and subsequent rates of crystallization between the two polymers would give rise to poor interfacial adhesion and even to the formation of gaps between the two phases because of the difference in level of shrinkage on termination of the crystallization process.[4] This difficulty can be alleviated, however, through compatibilization, that is, a mechanism for the formation of a diffused interlayer containing intimate mixtures of the two components.

Several studies have been reported in the literature on the use of a third polymer component to compatibilize PET/polyolefin blends. These include the use of an acrylic acid–grafted polypropylene to compatibilize blends of PET and polypropylene through the *in situ* formation of a compatibilizer resulting from transesterification reactions.[5]

Similar improvements in toughness for such blends have been reported with the use an ethylene–glycidyl methacrylate copolymer (EGMA),[6–10] whereas other workers have found polyolefin ionomers to be effective compatibilizers for these systems.[11–14] For the same purpose Mascia et al. used coionomeric mixtures of either ethylene acrylic acid or methacrylic acid copolymers with a polyhydroxyether (phenoxy).[4,15]

Toughening of PET by the direct addition of a functionalized polyolefin elastomer has been widely explored by a number of authors.[9,11,16,17] The most widely used toughening agents for thermoplastics are those rubbery polymers exhibiting an adequate level of compatibility to meet the specific requirements. To stabilize the morphology of the blend, the toughening component is often added directly as preformed particles with a core-and-shell structure. The core component is crosslinked to prevent their coalescence into larger particles, whereas the shell material is miscible with the polymer matrix to produce an interlayer that is well bonded to the two phases.

The addition of minor amounts of a rubbery polymer to a rigid polymer, however, can bring about a substantial reduction in modulus. The search for the means of preventing the deterioration of stiffness-related properties in the production of toughened polymers has stimulated considerable research interests in the use of rigid thermoplastic inclusions, as exemplified by the use of polysulfones and polyetherimides in epoxy resins.[18,19] Blends of rigid thermoplastics have also been studied, but without specific reference to toughness enhancement.[20] By matching the modulus of the two components it is possible to eliminate stress concentrations in the vicinities of the interface. This is beneficial in those cases in which the surrounding matrix is incapable of undergoing yielding, and in which toughness is enhanced through the formation of large surface areas resulting from crazing and phase delamination phenomena, but could be detrimental for systems relying on shear-induced yielding within the matrix to prevent the growth of cracks that lead to brittle fractures.

If the yield strength of the material forming the dispersed particles, however, is lower than that of the surrounding matrix, and the two phases are well bonded, the conditions will be created for the occurrence of microcavitations and particle tearing phenomena as mechanisms to relieve the local strain energy. However, this would also require that the dispersed particles be ductile under plane strain conditions. Such behavior cannot be expected from glassy thermoplastic polymers and can best be fulfilled by very ductile crystalline polymers, such as ultrahigh molecular weight polyethylene (UHMWPE) and polytetrafluoroethylene (PTFE). Both polymers are available in powder form and neither is prone to particle coalescence during mixing and subsequent processing, in view of their very high viscosity and also the high melting point in the case of PTFE. These features enable the dispersed particles to retain their particulate identity when mixed with other polymers.

Normally PTFE powders are used in polymeric compositions primarily as solid-state lubricants, where the poor adhesion between the particles and matrix is not so important, contrary to the requirement for toughness enhancement.

UHMWPE, on the other hand, has been used to a lesser extent as solid-state lubricants because of the rather larger particles of commercial products, that is, 50–150 μm as opposite to 1 μm or less for PTFE. However, because UHMWPE powders consist of agglomerates of very fine particles (Fig. 1), it should be feasible to separate them into its primary constituents.

The purpose of this work, therefore, is to explore the possibility of using conventional mixing operations to break up the aggregated particles of UHMWPE and to develop sufficient interfacial adhesion with PET as a means of providing an efficient toughening mechanism through any of

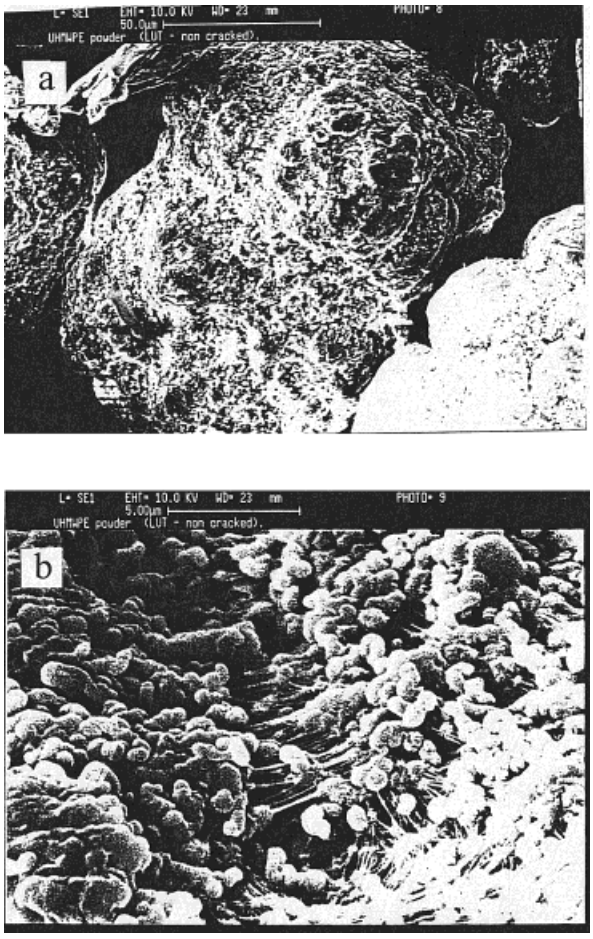

Figure 1 SEM micrographs of UHMWPE powder (Hostalen GUR 412; Hoechst,Germany): (a) Low magnification; (b) high magnification.

the usual expediencies, such as shear yielding within the matrix, particle tearing, and microcavitation.

EXPERIMENTAL

Materials

1. Ultrahigh molecular weight polyethylene (UHMWPE), Hostalen GUR 412 was from Hoescht (Germany). This has a weight-average molecular weight in the region of 4 $\times$ 10^6 g/mol.
2. Polyethylene terephthalate (PET), Tenite 10388, was from Eastman Chemical (Rochester, NY). This has a weight-average molecular weight in the region of 75,000 g/mol.
3. Acrylic acid, ferrous sulfate hexahydrate, triphenyl phosphine (TPP), and zinc acetyl acetonate monohydrate (ZnAcAc) were analytical grades supplied by Aldrich Chemicals (Milwaukee, WI).
4. Cycloaliphatic epoxy resin, Araldite CY 179 (Ciba Geigy, Summit, NJ), can be represented by the following formula:

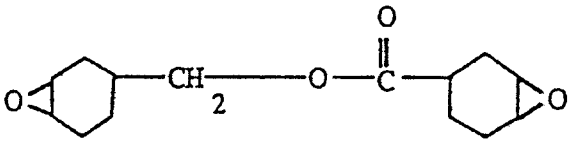

The UHMWPE powder was irradiated in the presence of air by γ-rays (Co^{60} source) at 1.0 kGy/h to total doses of 15 and 45 kGy. The powder was then allowed to stand for 24 h at room temperature and then stored in a freezer for up to 1 month before use. The surfaces of the primary particles of the irradiated powder were subsequently surface grafted with acrylic acid and refunctionalized according to the procedure described below.

To deliver the acid to the inner surfaces of the agglomerated secondary particles, which is required for the grafting reactions, experiments were carried out both on a small scale ($\sim$ 50 g), using a high-speed mixer, and on a large scale ($\sim$ 1 kg) in a stirred flask from a more dilute solution.

In either case the reactions involved were as follows:

1. Grafting with an aqueous acrylic acid solution to different levels.
2. Functionalizing the epoxy group by reacting the acid-grafted product with an excess of the difunctional cycloaliphatic epoxy resin.
3. Ionizing the acid groups by the formation of zinc salts through the addition of ZnAcAc.

The epoxy/acid reaction is expected to take place in accordance with the mechanism as shown in Scheme 1.

The neutralization reaction is expected to take place according to Scheme 2.

In the small-scale experiments the first step of the grafting reaction, involving the deposition of the acid on the surface of the inner primary particles, was carried out by mixing the powder with

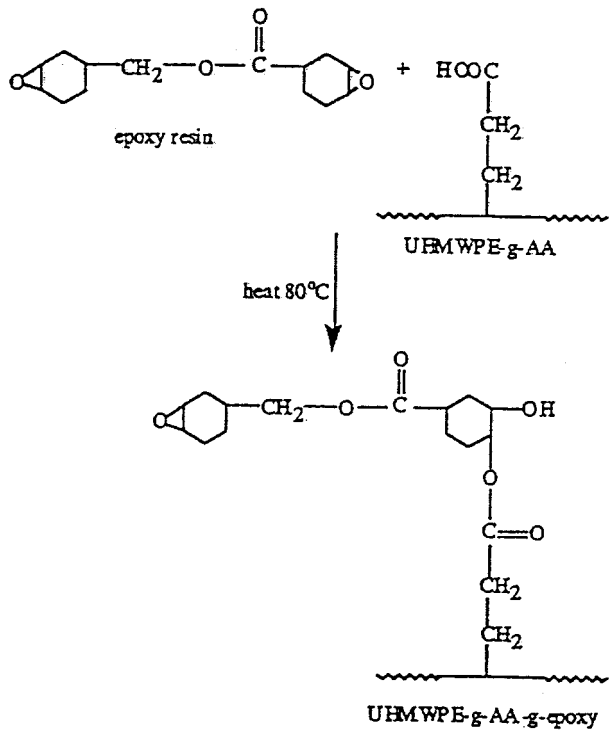

Scheme 1

an aqueous acrylic acid solution for 10 min in a small high-speed mixer (adapted from an electrically driven coffee grinder). This was then transferred to a lidded flask, which was then heated for 5 h at 80°C in an oven. The weight ratio of powder to aqueous monomer solution was 80/20 and the acid concentration in the water solution was 80%. Small amounts of ferrous sulfate (i.e., 21 mg, equivalent to 0.042 wt %) were added to the solution to inhibit homopolymerization reactions.

The epoxidation reaction was carried out by mixing the acid-grafted powder with a 50% solution of the cycloaliphatic epoxy resin in methyl ethyl ketone (MEK) in a high-speed mixer for 10 min, using amounts corresponding to a molar ratio of acid/epoxy groups of 1 : 2.2. The reaction was catalyzed with 1 wt % TPP, with respect to the epoxy resin content.

The mixture was subsequently heated in a closed container at 80°C for 18 h and washed with large quantities of MEK to remove the unreacted resin residues, and then dried in an oven at 80°C.

The acid neutralization reaction was carried out in a stirred flask adding 36 g powder to 400 mL of a zinc acetyl acetonate solution in ethanol (5 wt %) and heated for 18 h at 80°C. The suspension was filtered and washed several times with methanol.

The grafted and functionalized UHMWPE powder was mixed with predried PET at a 10 wt % level (i.e., ratio PET/UHMWPE = 90/10) using a 65-mL Haake mixer at 270°C and operating with a rotor speed of 75 rpm. To minimize the extent of thermal oxidation during mixing, the chamber was purged with nitrogen prior to being filled with polymer and kept under a nitrogen

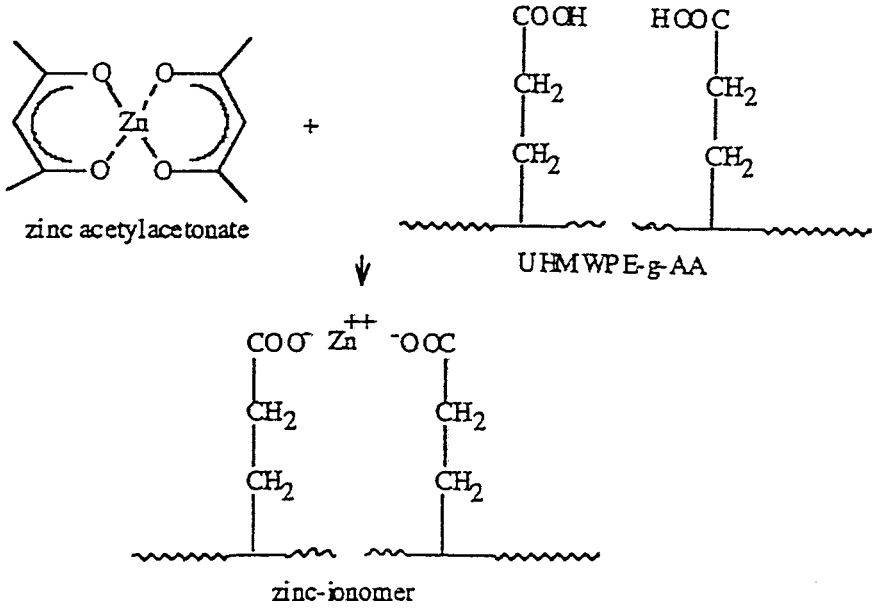

Scheme 2

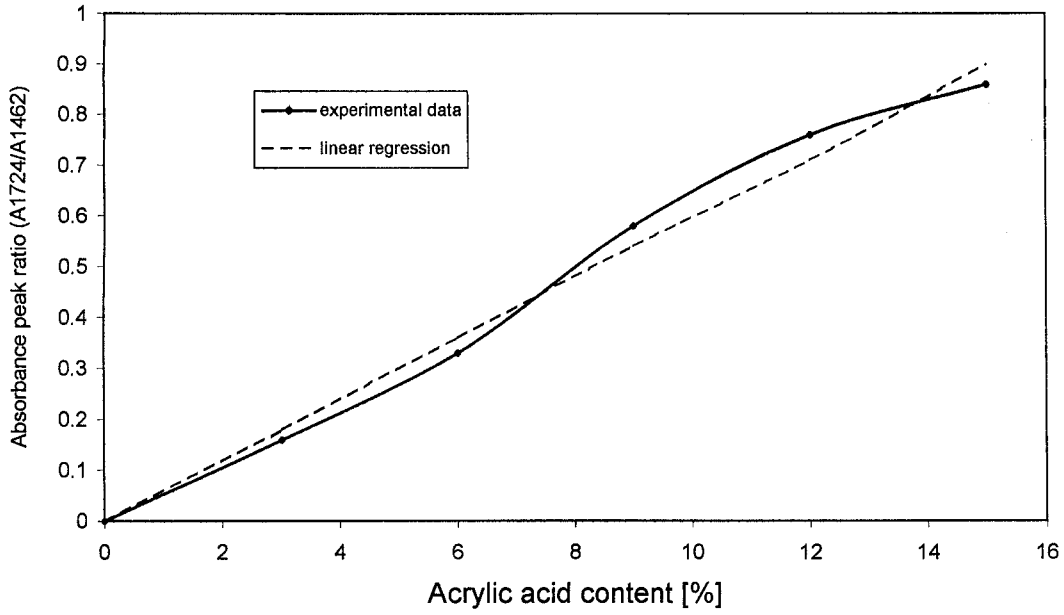

Figure 2 Calibration curve (absorbance ratio CO/CH_2) for the amount of acrylic acid adsorbed on UHMWPE powder.

blanket during the entire 15-min mixing cycle. The torque registered during mixing was monitored and the final equilibrium value was used for comparisons.

For the large-scale experiments the deposition of the acrylic acid on the internal surface of the powder and the subsequent grafting reaction was carried out in a 15-L high-speed mixer (model TRV 25; T. K. Flieder) at 80°C for 1 h, using 2 kg of irradiated powder and 400 mL of 20% acrylic acid solution in water, containing 0.448 g ferrous sulfate.

The reaction mixture was then washed separately with hot water and dried in flat trays for 5 h using an oven at 80°C.

The ionization reaction, washing, and drying procedures were carried out as described previously using 250 mL of ZnAcAc solution (28.2 wt %) for 1 kg of powder.

The epoxide functionalization of the powder was carried out in the 15-L Flieder high-speed mixer at 80°C for 5 h using a 50 wt % solution of CY 179 epoxy resin in MEK, containing 1 wt % TPP. The grafted powder was then washed in MEK to remove the unreacted epoxy resin and dried in an oven at 80°C. The weight ratio of powder to monomer solution was 82.4/17.6.

Control experiments were carried out using both pristine and irradiated UHMWPE powders.

The predried PET granules and the UHMWPE powders were mixed at 90/10 weight ratio in an APV twin-screw extruder (model MP30TC) at 270°C. The screw configuration was made up according to the manufacturer's recommendation and was operated in a starved mode to give an output of 10 kg/h and a head pressure of 1.75 MPa.

Structure Characterization

The quantitative analysis of the UHMWPE powder after irradiation and subsequent grafting and functionalization reactions was carried out by diffusion reflectance spectroscopy (DRIFT) using a Mattson 3000 FTIR spectrometer. A calibration curve was first obtained by recording the absorbance of characteristic groups (i.e., COOH and CH_2) on mixtures of acrylic acid and UHMWPE. A typical calibration curve produced by FTIR, using the DRIFT method, is shown in Figure 2 in the form of a plot of the ratio of the absorbance for the C═O stretching vibration of acid groups at 1724 cm^{-1} to the absorbance at 1462 cm^{-1}, corresponding to the CH_2 group bending deformation of the polyethylene backbone. Experiments were carried out in duplicate and in all cases the difference between the data obtained was not more than 10%.

The morphology of the blends was examined on fracture surfaces using a scanning electron microscope (Cambridge Stereoscan 360 System; Cambridge Biotech, Rockville, MD) and the level of

crystallinity for the two polymer components was assessed by thermal analysis using a Du Pont DSC 2000 apparatus (Du Pont, Wilmington, DE), with heating and cooling rates both set at 20°C/min.

The molecular weight of the polyester component was determined by gel permeation chromatography after extraction to remove the UHMWPE phase. These measurements were carried out in the research laboratories of Eastman Chemical at Kingsport, TN.

Preparation and Testing of Specimens

The mixtures produced on the Haake mixer were compression-molded into plaques (90 × 90 × 0.5 mm) at 270°C and quenched under pressure. These were punch-cut into dumbbell-shaped specimens with a waist of 3 mm and a gauge length of 30 mm. The specimens were annealed at 130°C for 5 h to maximize the level of crystallinity and were then tested in tension at room temperature, using a JJ Lloyd 1000S tensile-testing machine with a clamp separation speed of 5 mm/min.

The mixes produced on the twin-screw extruder were injection-molded into tensile specimens (ASTM D638) and rectangular bars (52 × 13 × 6 mm), using a Negri Bossi (model NB 62) injection-molding machine. The latter were milled down to 4 mm thickness to remove the sink marks from both sides of the specimens. Half of the specimens were annealed at 130°C for 5 h.

The nonannealed (amorphous) specimens were tested in tension at 80 and 100°C on a JJ Lloyd tensile-testing machine with a cross-head speed of 500 mm/min. The annealed (crystalline) rectangular specimens were tested at room temperature in a three-point bending mode to measure the flexural modulus and the fracture toughness parameter K_{IC}, known as the critical stress intensity factor, that is,

$$K_{IC}=Y\sigma_0 a^{-1/2}$$

where Y is the compliance calibration factor, a is the crack length, and σ_0 is the nominal stress applied (not allowing for the length of a crack).

Single-edge notch (SEN) specimens with different crack lengths, varying from 2.4 to 6.2 mm and a notch tip radius of 0.25 mm, were used to measure K_{IC}. In this case the expression for K_{IC} can be written as

$$K_{IC}=Y''P^*/BW^{1/2}$$

where Y'' is a derived compliance calibration factor (which incorporates the ratio a/W), P^* is the load to fracture, and B and W are the thickness and width of the specimen, respectively.

The testing speed was set at 5 mm/min for both flexural modulus and fracture toughness measurements. The span-to-thickness ratios were, respectively, 20 : 1 for the flexural tests and 4 : 1 for the fracture toughness measurements. The flexural modulus was calculated from the slope of the linear portion of the force/extension curve, whereas the fracture toughness parameter K_{IC} was obtained from the slope of the plots $P^*/BW^{1/2}$ against $1/Y''$. (The values of Y'' were obtained from Ref. 21.)

However, the fracture toughness is more usefully expressed in terms of energy requirements for crack propagation, based on the concept of critical strain energy release rate G_{IC}, defined as the rate of change in strain energy per infinitesimal increase in crack length a for a given specimen thickness (i.e., $\delta U/B\ \delta a$). Hence, the results of the fracture toughness tests were converted to G_{IC} values, using the relationship $K_{IC}^2/E = G_{IC}$, where E is the Young's modulus. In this case the value of E was equal to flexural modulus, even though this may be subjected to some errors arising from the differences in strain rate in the two respective tests.

In all cases five specimens were used for each test carried out and the average was taken to work out the quoted results. The estimated error for the data reported is less than 15%.

RESULTS AND DISCUSSION

The micrographs in Figure 1 show details of the UHMWPE powder, which clearly reveal the presence of primary particles in the region of 0.5–2 μm aggregated within densified secondary particles about 100 μm in diameter. The BET surface area measured for these particles was 1.932 m^2/g. It is possible, however, that the degree of compactness of densified secondary particles may depend on the conditions that the manufacturer uses in the removal of the solvent after polymerization. The UHMWPE grade obtained from the United States contained particles with a distinct solid skin over several regions of the particle surface. The BET surface area of these particles was correspondingly considerably lower than the corresponding polymer grade obtained from Europe, that is, 0.6566 m^2/g compared with 1.9320 m^2/g.

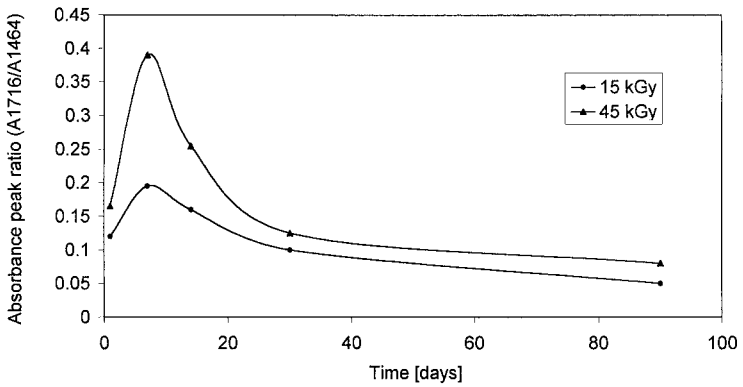

Figure 3 Absorbance ratio CO/CH_2 for UHMWPE powder as a function of storage time after irradiation at 15 and 45 kGy.

The diagrams in Figures 3 and 4 illustrate the changes in peak absorbance ratios for C═O stretching to CH_2 bending deformation (A1716/A1462) and COO^- asymmetric stretching/CH_2 (A1590/A1462) that take place during storage of the UHMWPE powder at room temperature after irradiation.

The breaking up of the particle agglomerates into primary particles is an indirect evidence that reactions have occurred during blending between the functional groups on the surface of the UHMWPE particles and the surrounding PET. The resulting strong interfacial bonding, in fact, provides an efficient stress-transfer mechanism for the breaking up of the secondary particle aggregates by virtue of the fact that the functional groups on the fresh surfaces emerging from the cleavage of an agglomerated particle will further react with the surrounding PET molecules, thereby creating an accelerated mechanism for the comminution of the conglomerates into the primary discrete particles. The reaction of the epoxy groups and the carboxylate anions with PET are expected to be ionically induced transesterification reactions, whereas those for the irradiated powder are likely to be primarily free radical in nature, causing cleavage of the CH_2—COO. The identified carboxylate anions (Fig. 3) are also expected to participate in the reactions in the same way as the ionized carboxylic acid functionality introduced by surface grafting of acrylic acid.

In Table I is reported the degree of acrylic acid grafting (wt %) obtained by the two procedures used to carry out the grafting reactions. The data show that the reaction carried out in the stirred flask using large quantities of acrylic acid solution (i.e., 20 polymer/80 solution) produces higher yields of grafted monomer. In Table II are reported the yields of the epoxide functionalization reaction for the various grafted powders. These demonstrate that the epoxidation reactions are

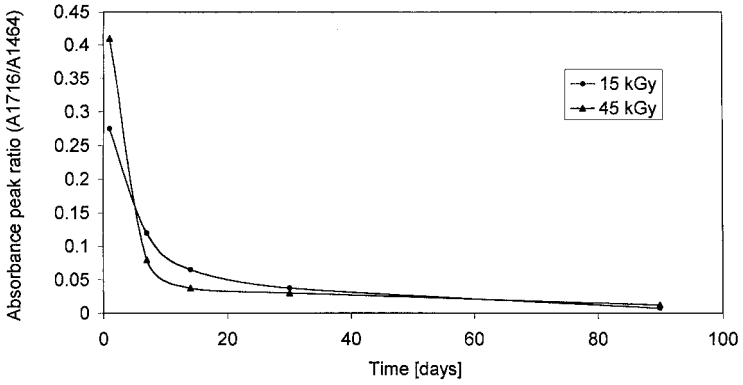

Figure 4 Absorbance ratio COO^-/CH_2 for UHMWPE powder as a function of storage time after irradiation at 15 and 45 kGy.

Table I FTIR Data for Grafted Acrylic Acid for the Two Experimental Procedures

Monomer in Water Solution (wt %)	Reaction Time at 80°C after Mixing (h)	Absorbance Ratio at 1724/1462 cm^{-1}	Acrylic Acid Grafted (%)
Small-scale/high-speed mixing method			
20	1	0.13	3.5
20	5	0.11	3.0
60	1	0.13	5.1
60	5	0.12	5.3
Large-scale/stirred reactor method			
5	3	1.25	20.8
10	3	1.15	19.1
30	6	1.07	17.8

also more efficient when the acrylic acid grafting is carried out in a stirred flask with large quantities of monomer solution. In Table III are reported the FTIR data and the calculated ionization efficiency for the formation of zinc carboxylate groups in the reaction with ZnAcAc. These indicate that, in general, the yield for the zinc salt formation was much lower than that of the epoxidation reactions.

In Figure 5 are shown the data recorded on the torque rheometer in the mixing of PET with UHMWPE powder subjected to various chemical treatments after irradiation. The blends with the untreated powder gave the lowest torque, whereas the powder irradiated to 45 kGy gave the highest value, followed closely by those containing the zinc carboxylate powder. This is indicative of a more efficient mechanism for the transfer of stresses in the mixing process from the low-viscosity PET matrix to the "rubbery" UHMWPE particles, which results into a higher "blend viscosity" resulting from the formation of smaller and well-dispersed particles. Although the data reported are for one experiment the differences are very large and much greater than the variations normally expected for this type of experiment.

The SEM micrographs in Figure 6, taken on the surface of fractured tensile specimens produced from the compression-molded plaques, show that the particles of untreated UHMWPE powder and those grafted with acrylic acid within the PET matrix are not much smaller than the original aggregates. The samples that were only irradiated and those containing zinc carboxylate grafts, on the other hand, display a complete

Table II FTIR Data for the Epoxidation of Acrylic Acid Grafts

Monomer in Water Solution (wt %)	Reaction Time at 80°C after Mixing (h)	Absorbance Ratio at 902/1895 cm^{-1}		Epoxidation Efficiency[b] (%)
		D_1[a]	D_2[a]	
Small-scale/high-speed mixing method				
20	1	1.059	0.053	29
20	5	1.114	1.123	42
60	1	1.089	0.229	54
60	5	0.947	0.15	46
Large-scale/stirred reactor method				
5	3	1.514	0.451	64
10	3	1.471	0.662	76
30	6	1.556	0.451	63

[a] D_1 = absorbance ratio value after washing with MEK to remove unreacted epoxy resin; D_2 = absorbance ratio value before washing with MEK.

[b] Epoxidation efficiency (X%) is obtained from the expression $X = 2D'/(1 + D')$, where $D' = D_1/D_2$. The rationale is that one epoxy group will react so that $D_2 \propto X$ and $D_1 \propto 2(1 - X) + X = 2 - X$. Hence $D' = X/(2 - X)$ and $X = 2D'/(1 + D')$.

Table III FTIR Data for the Zinc Ionomerization of Acrylic Acid Grafts

Mixing/Reaction Time at 80°C (h)	Absorbance Ratio at 1720/1464 cm^{-1}		Ionization Efficiency[b] (%)
	D_1[a]	D_2[a]	
Low-level grafting: small-scale/high-speed mixing method			
0	0.132		
1		0.111	16
3		0.095	28
5		0.090	32
High-level grafting: large-scale/stirred reactor method			
0	1.253		
1		1.140	9
3		0.927	26
5		0.777	38
18		0.752	40

[a] D_1 and D_2 are the absorbance ratios before and after the ionomerization reaction.

[b] Obtained from the expression $Y = 1 - D_2/D_1$.

breakdown of the aggregates into their primary particles (Fig. 7). It is interesting to note that the samples containing the epoxidized grafts reveal the presence of highly drawn particles strongly bound to the surrounding PET matrix (Fig. 8). This is indicative of a stronger adhesive bond between the UHMWPE particles and the surrounding PET matrix. Hardly any particles, in fact, are seen to be debonded from the matrix, contrary to the other cases.

The thermal data in Table IV suggest that the blends containing the epoxidized UHMWPE powder display a slightly lower heat of fusion for the PET phase. The tests were carried out in duplicate and the differences were found to be consistent to render the comparison valid for the purpose of the analysis. The associated reduction in level of crystallinity is reflected also in the lower modulus value for this blend (see later and data in Table VI). Although there is no direct evidence, it is possible to deduce that the PET immediately adjacent to the surface of the particles could have an even lower level of crystallinity than the average for the entire matrix as a result of the formation of chemical bonds at the interface, which restrict the molecular motions required for the crystallization. This is quite the opposite of what would happen for the case in which the surface of the UHMWPE particles contain ions, given that these are known to act as nucleating sites for the crystallization of PET.[15] This is confirmed by the the thermal data in Table IV, showing that the heat of fusion of the PET increases when the acrylic acid grafts are partially neutralized by the reaction with ZnAcAc. Once more the duplicated tests consistently showed a distinct difference between the two sets of data. It is also possible that the carboxylate anions formed by the irradiation-

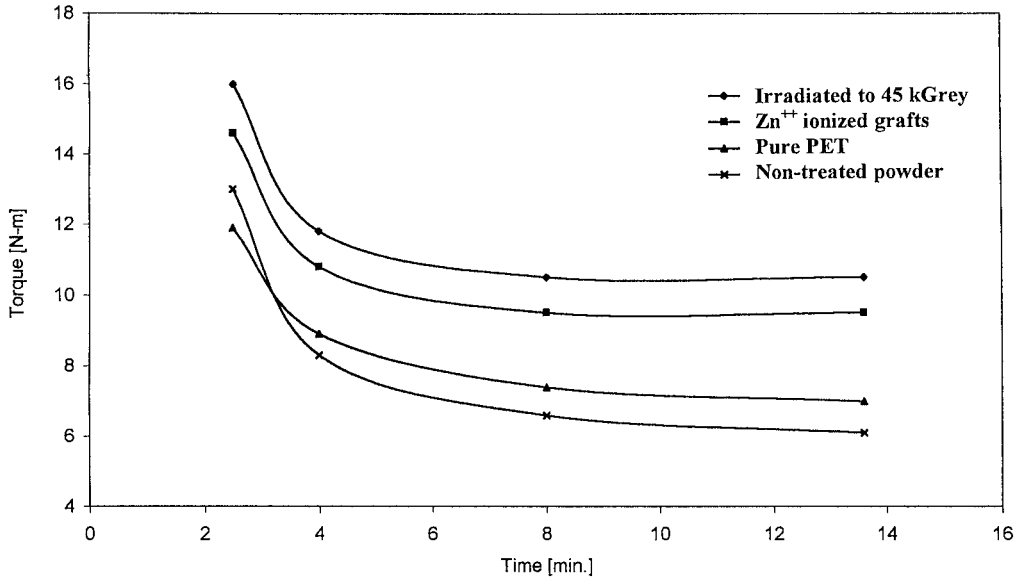

Figure 5 Torque recorded during mixing of PET and UHMWPE powder in the Haake rheometer at 275°C and 75 rpm.

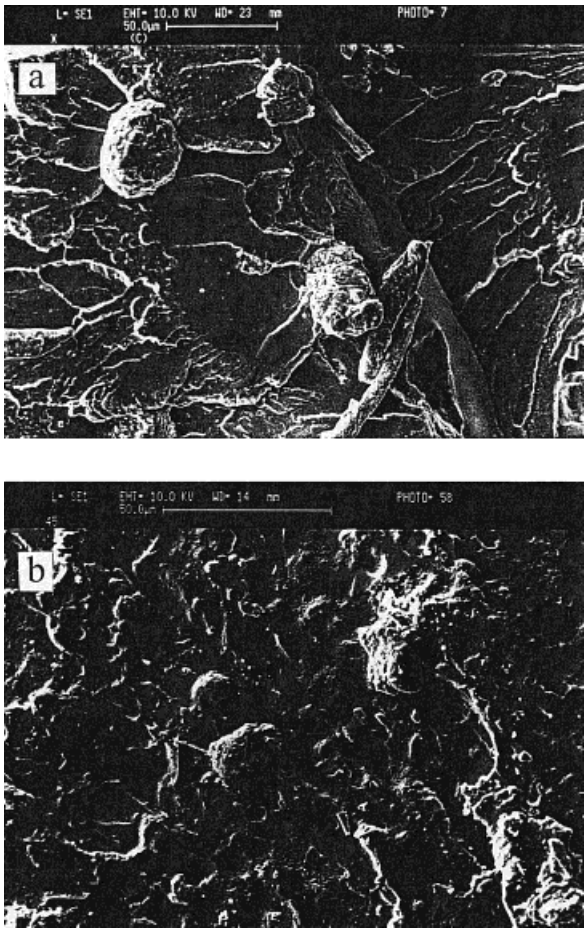

Figure 6 SEM micrographs of PET/UHMWPE blends: (a) Untreated powder; (b) powder grafted with acrylic acid (high level of grafting).

induced oxidation at the surface of the UHMWPE particles have a similar effect on the samples in which the powder was irradiated only before blending with PET.

At the onset of yielding the more amorphous nature of the PET interfacial layer for the blends containing epoxidized powder creates the required conditions for shear yielding, in favor of the formation of cracks within the matrix. The fact that this particle-tearing type of fracture mechanism does not appear to bring about a very significant increase in ductility (Table V) and toughness (Table VI) may be indicative of the relatively low contribution to energy dissipation by the crack bridging effect of the cold-drawn UHMWPE particles, relative to shear yielding within the matrix or interfacial microcavitations and delaminations prior to the occurrence of fracture. The error band for all the data displayed in these tables is not greater than 10%; hence, the observed differences can be considered to be statistically significant.

In Table V are shown the results of the tensile tests on the annealed samples. From these it evident that both tensile strength and elongation at break are highest for systems in which the particle conglomerates of UHMWPE have broken down into primary particles during mixing. For the yield strength the values are, respectively, 65.2 versus 42.2 MPa, and for the elongation at break the values are 10.1 versus 4.4 or 3.8%. At the same time the thermal data in Table IV show that, in these cases, the level of crystallinity for the PET matrix is also higher, except for that of blends produced with the epoxidized powder, as explained earlier. The differences observed for different samples were found to be reproducible in duplicated tests.

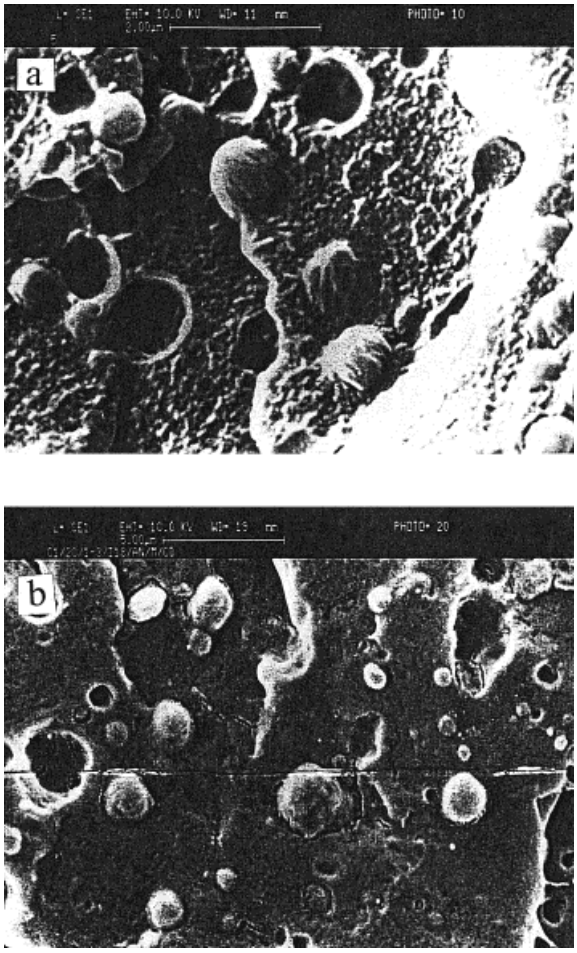

Figure 7 SEM micrographs of PET/UHMWPE blends: (a) Powder irradiated at 45 kGy; (b) powder grafted with acrylic acid (5.3%) and ionized with ZnAcAc.

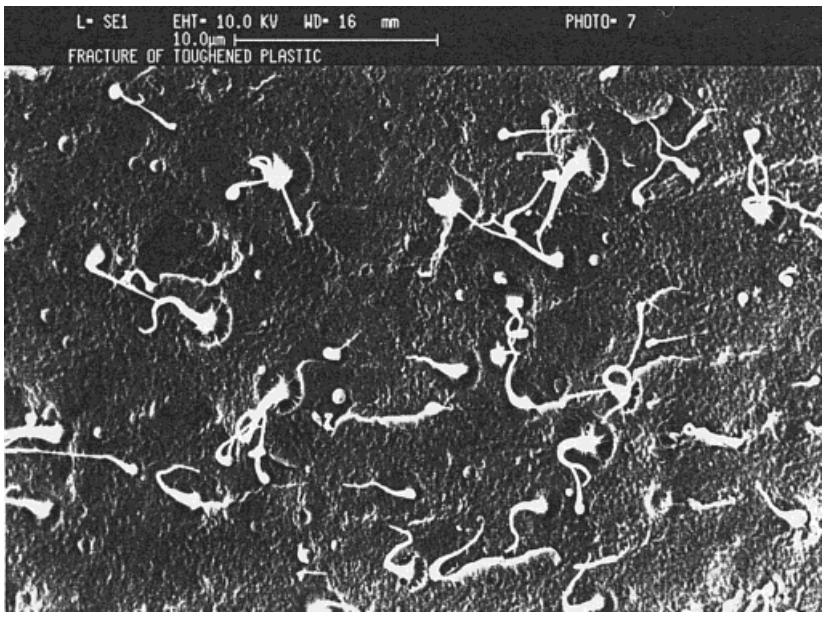

Figure 8 SEM micrographs of PET/UHMWPE blends produced from UHMWPE powder grafted with acrylic acid (5.3%) and functionalized with epoxy groups.

The higher level of crystallinity, however, cannot be considered to be the cause for the increase in elongation at break, but only a consequence of the higher nucleation efficiency of the smaller UHMWPE particles for the crystallization of the surrounding PET matrix. Hence the enhanced ductility must be attributed to the presence of smaller UHMWPE particles well bonded to the surrounding PET matrix.

An indication of the occurrence of plastic deformations for the more ductile samples is obtained from an inspection of the stress/strain curves in Figure 9. Similar improvements were found for the mechanical properties of the samples produced by the large-scale procedure (Table VI). Particularly significant is the observation that the G_c values for the samples containing the irradiated UHMWPE powder are about 10-fold

Table IV DSC Data for Crystalline PET/UHMWPE Blends (90/10 Weight Ratio)[a]

Powder Treatment/Composition	T_m[b] (°C)	ΔH_f[c] (J/g)	T_c[d] (°C)	ΔH_c[e] (J/g)
N.A./pure PET	249.6	37.5	181.1	35.9
Nontreated	250.2	33.4	189.5	31.8
Irradiated @ 15 kGy	251.6	39.6	174.8	30.3
Irradiated @ 45 kGy	252.2	41.5	185.1	39.8
3.5% Grafted acrylic acid	250.1	33.8	188.5	32.6
3.5% Grafted acrylic acid followed by epoxidation	251.1	38.8	189.2	37.4
3.5% Grafted acrylic acid followed by ionomerization	250.5	43.3	179.4	41.5
5.3% Grafted acrylic acid	251.4	34.6	189.9	33.5
5.3% Grafted acrylic acid followed by epoxidation	251.3	38.9	175.7	32.2
20.8% Grafted acrylic acid	251.8	37.4	179.9	31.4
20.8% Grafted acrylic acid followed by ionomerization	251.2	42.7	181.4	40.6

[a] Samples were produced by injection molding and then annealed.
[b] T_m = melting point.
[c] ΔH_f = first cycle heat of fusion.
[d] T_c = cooling cycle crystallization temperature.
[e] ΔH_c = heat of crystallization in cooling cycle.

Table V Mechanical Properties of Crystallized PET/UHMWPE Blends at 90/10 Weight Ratio Based on UHMWPE Powders with Different Treatments and Surface Reactions[a]

Powder Treatment/Composition	Young's Modulus (GPa)	Stress at Yield (MPa)	Elongation at Yield (%)	Stress at Break (MPa)	Elongation at Break (%)
N.A./pure PET	2.08	n.a.	n.a.	66.3	4.1
Nontreated	1.75	n.a.	n.a.	42.2	4.4
Irradiated @ 15 kGy	1.83	62.3	7.0	61.1	10.1
Irradiated @ 45 kGy	1.85	61.5	6.7	58.9	8.9
3.5% Grafted acrylic acid	1.77	n.a.	n.a.	43.3	4.2
3.5% Grafted acrylic acid followed by epoxidation	1.79	60.4	6.1	59.9	7.8
3.5% Grafted acrylic acid followed by ionomerization	1.83	65.2	5.8	64.5	7.2
5.3% Grafted acrylic acid	1.82	n.a.	n.a.	41.5	3.2
5.3% Grafted acrylic acid followed by epoxidation	1.77	58.6	6.5	54.2	8.2
20.8% Grafted acrylic acid	1.79	n.a.	n.a.	38.9	3.8
20.8% Grafted acrylic acid followed by ionomerization	1.81	63.2	5.2	60.8	6.4

[a] Specimens were produced by compression-molded plaques.

higher than those produced with the untreated powder. In parallel to this, the K_c values are more than fourfold higher, and the flexural strength nearly twice as high.

The data reported in Table VII show that compounding and processing of the materials have induced, in all cases, a considerable reduction in the molecular weight of the PET matrix. This is approximately the same for all the blends and also for the pure PET samples, and suggests that this is entirely related to the hydrolytic decomposition imposed by the process rather than the nature of the powder used, even though the samples produced from the nontreated powders appear to have undergone a slightly higher level of degradation.

Another significant effect of the disaggregation of particles is demonstrated by the tensile stress/extension ratio curves obtained at 80 and 100°C for the nonannealed samples, which are shown in Figure 10. Higher yield stress and elongation at break values are displayed by the samples in which the UHMWPE particles have been disintegrated as a result of the powder treatments, thus resulting in a more efficient reinforcement for the amorphous PET matrix. The presence of these fine UHMWPE particles, however, reduces the level of strain hardening during drawing, but it is

Table VI Fracture Toughness and Flexural Test Data for Crystalline PET/UHMWPE Blends (90/10 Weight Ratio) for Injection-Molded Specimens

Powder Treatment/Composition	Crystallinity (%)	$E_{(F)}$[a] (GPa)	$\sigma_{(F)}$[b] (MPa)	K_c[c] (MN/m$^{3/2}$)	G_c[d] (kJ/m^2)
PET (as received)		1.95	94.1	2.7	3.6
PET (extruded)	29.1	1.71	77.8	1.4	1.1
Nontreated	27.0	1.53	56.8	0.8	0.4
Irradiated @ 15 kGy	26.7	1.55	90.3	3.6	8.4
Irradiated @ 45 kGy	27.4	1.59	86.8	3.3	6.7
3.5% Grafted acrylic acid followed by epoxidation	25.9	1.43	70.9	2.8	5.5
3.5% Grafted acrylic acid followed by ionomerization	28.8	1.49	70.8	2.5	4.2

[a] $E_{(F)}$ = flexural modulus.
[b] $\sigma_{(F)}$ = flexural strength.
[c] K_c = critical stress intensity factor.
[d] G_c = critical strain energy release rate.

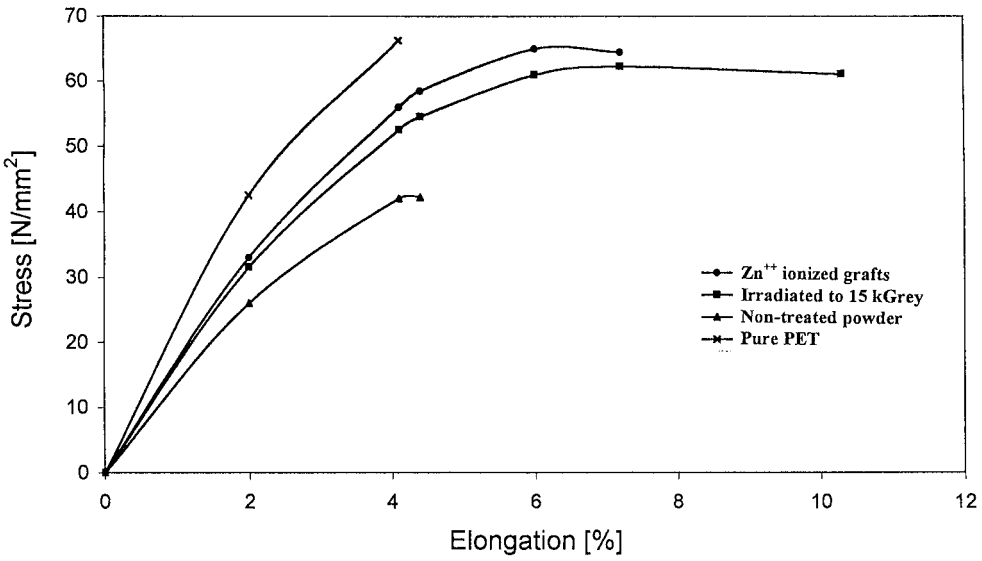

Figure 9 Typical stress/strain curves for annealed PET/UHMWPE blends based on powders subjected to different surface treatments.

difficult to ascertain whether this results from a reduction in the rate of strain-induced crystallization of the PET matrix or whether the reinforcing effect of the UHMWPE particles is reversed as a result of the increased modulus of the crystallizing PET matrix.

CONCLUSIONS

The main conclusions that can be drawn from this work are:

1. Functionalization of the surface of primary particles in commercial UHMWPE powders with either free radicals, glycidoxyl groups, or metal carboxylate ions is an effective way of breaking up the particle agglomerates in blends with PET.
2. The breaking up of particle agglomerates, caused by interfacial reactions with the surrounding PET matrix, brings about an effective dispersion of the primary particles and a large increase in ductility and toughness in the resulting blends in their crystalline state.
3. The use of glycidoxyl functionalized powders provides an extremely strong bond with the PET matrix and results in a fracture mechanism involving extensive cold drawing of the UHMWPE dispersed particles.

Table VII Molecular Weight Data for the PET Matrix Obtained on Extruded Pellets of PET/UHMWPE Blend (90/10 Weight Ratio)

Powder Treatment/Composition	Number-Average Molecular Weight [M_n] (mol/g)	Weight-Average Molecular Weight [M_w] (mol/g)	M_w/M_n
PET (as received)	35,000	75,200	2.15
PET (extruded)	18,258	43,202	2.37
Nontreated	17,452	42,249	2.42
Irradiated @ 15 kGy	18,817	45,397	2.41
Irradiated @ 45 kGy	18,654	45,203	2.43
3.5% Grafted acrylic acid followed by epoxidation	18,594	43,492	2.34
3.5% Grafted acrylic acid followed by ionomerization	18,476	45,640	2.46

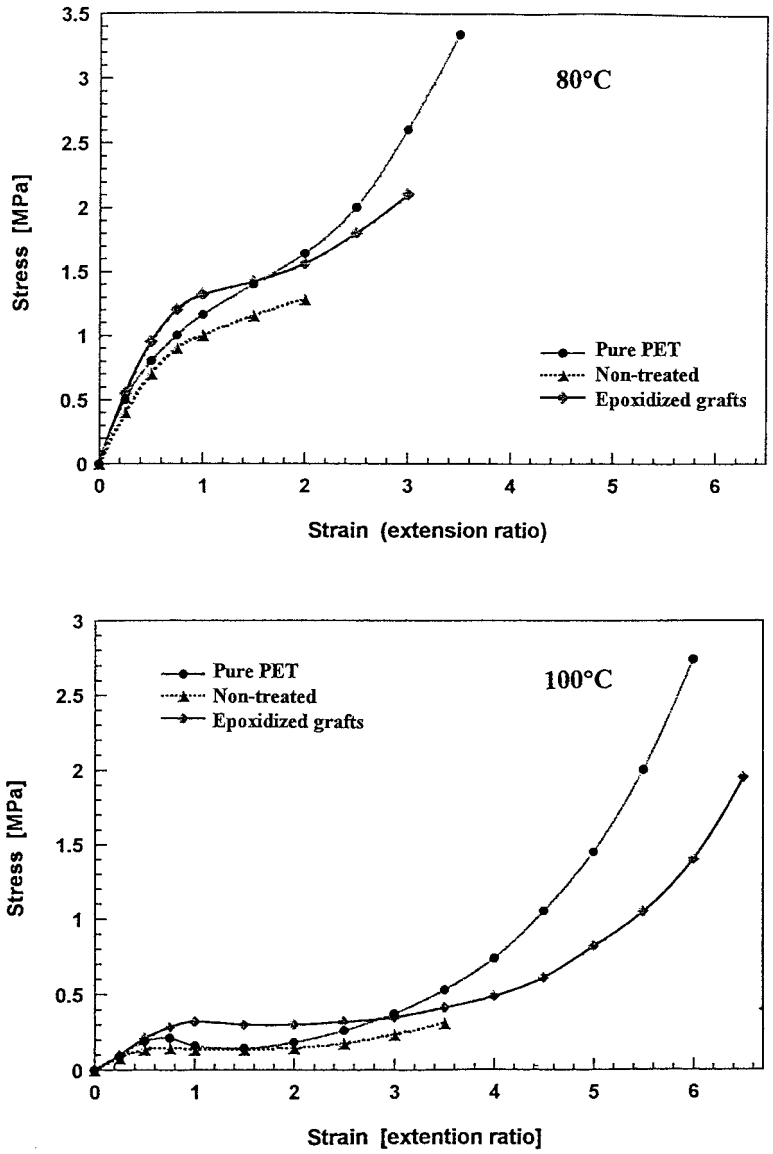

Figure 10 Curves for nominal stress versus extension for PET/UHMWPE blends recorded in tensile tests at high temperatures.

The authors acknowledge the financial support obtained by Eastman Chemical Company and thank the staff in the analytical section for their assistance with the molecular weight measurements of the PET matrix in various blends produced in this work.

REFERENCES

1. Deyrup, E. J. in High Performance Polymers: Their Origin and Development; Seymour, R. B.; Kirkshenboum, G. S., Eds.; Elsevier: New York, 1986; pp. 81–94.
2. Pillon, L. Z.; Lara, I. Polym Eng Sci 1984, 24, 1300.
3. Kamal, M. R.; Shato, M. A. Polym Eng Sci 1982, 22, 1127.
4. Mascia, L.; Moggi, A. J Polym Sci Part B Polym Phys 1993, 31, 1309.
5. Bataille, P.; Boisse, S. Polym Eng Sci 1987, 33, 827.
6. Kamdor, K. M.; Dagli, S. S. in ANTEC '93, 9–13 May 1993, New Orleans, LA; p. 1249.
7. Akkapeddi, M. K.; Van Bustrik, Polym Mater Sci Eng 1992, 67, 317.
8. Riiter, M.; Markku, T. M.; Seppela, J. V. J Appl Polym Sci 1995, 57, 573.

9. Epstein, B. N. (to DuPont) U.S. Pat. 4,172,859, 1979.
10. Loivier, E. J. (to Copolymer Rubber and Chemical Co.) U.S. Pat. 4,594,386, 1986.
11. Kalfoglou, N. K.; Skafidas, D. S. Polymer 1994, 35, 3624.
12. Kalfoglou, N. K.; Skafidas, D. S. Eur Polym J 1994, 30, 933.
13. Joshi, M.; Misra, A. J Appl Polym Sci 1991, 43, 311.
14. Joshi, M.; Misra, A. J Appl Polym Sci 1992, 45, 1837.
15. Mascia, L.; Bellahdeb, F. Adv Polym Technol 1994, 13, 99.
16. Penco, M.; Pastorino, M. A.; Occhiello, E. J Appl Polym Sci 1995, 57, 329.
17. Chen, I.-M.; Shiah, C.-M. in ANTEC '89, 1–4 May 1989, New York; p. 1802.
18. Hedrick, J. L.; Wilgor, I.; Jurek, M.; Hedrick, J. C.; Wilkes, G. L.; McGarth, J. E. Polymer 1991, 32, 2920.
19. Yoon, T. H.; Liptak, S. C.; Priddy, D.; McGarth, J. E. in ANTEC '93, 9–12 May 1993, New Orleans, LA; p. 3011.
20. Mascia, L.; Martin, L. H. High Perf Polym 1996, 8, 119.
21. Mascia, L.; Hashim, K. Colloid Polym Sci 1997, 275, 689.
22. Brown, W. F., Jr.; Srawley, J. F. ASTM Spec Tech Publ 1966, 410, 12.